Supplementary Information

of

Probiotics functionalized with a gallium-polyphenol network modulate the intratumor microbiota and promote anti-tumor immune responses in pancreatic cancer

Zi-Yi Han, Zhuang-Jiong Fu, Yu-Zhang Wang, Cheng Zhang, Qi-Wen Chen, Jia-Xin An, Xian-Zheng Zhang*

Key Laboratory of Biomedical Polymers of Ministry of Education and Department of Chemistry, Wuhan University, Wuhan 430072, P. R. China

*Corresponding author, E-mail: xz-zhang@whu.edu.cn

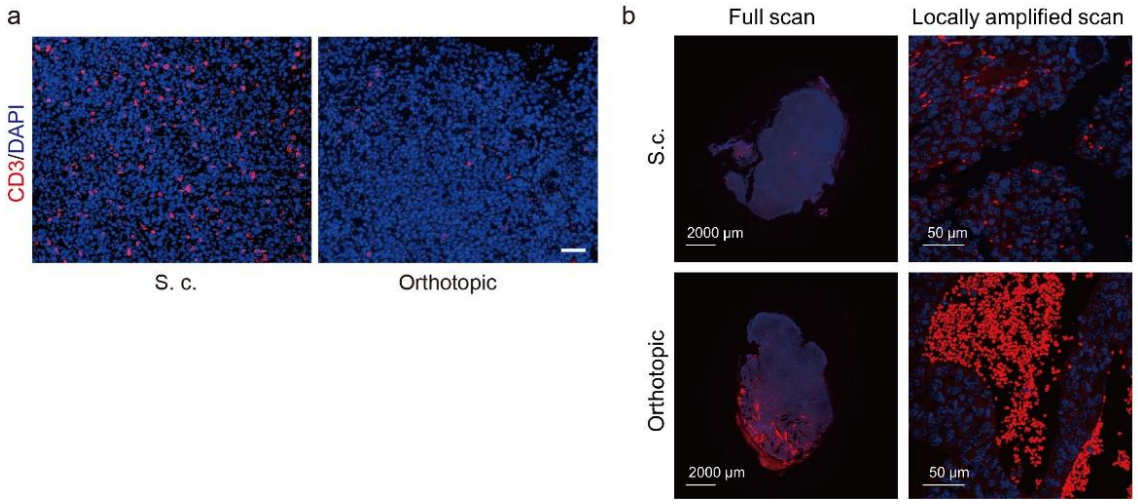

Supplementary Fig. 1 Intratumour microbiota analyses. a Intratumor T cell infiltration demonstrated by CD3-immuno-fluorescence staining in subcutaneous (S.c.) and orthotopic PDAC mice. The scale bar is 50 μm. Experiments were repeated three times. $n = 9$ mice in each group. **b** Intratumor microbes demonstrated by FISH staining in S.c. and orthotopic PDAC mice. Both full scan and locally amplified scan were showed (The bacteria were stained into red). Experiments were repeated three times. $n = 9$ mice in each group.

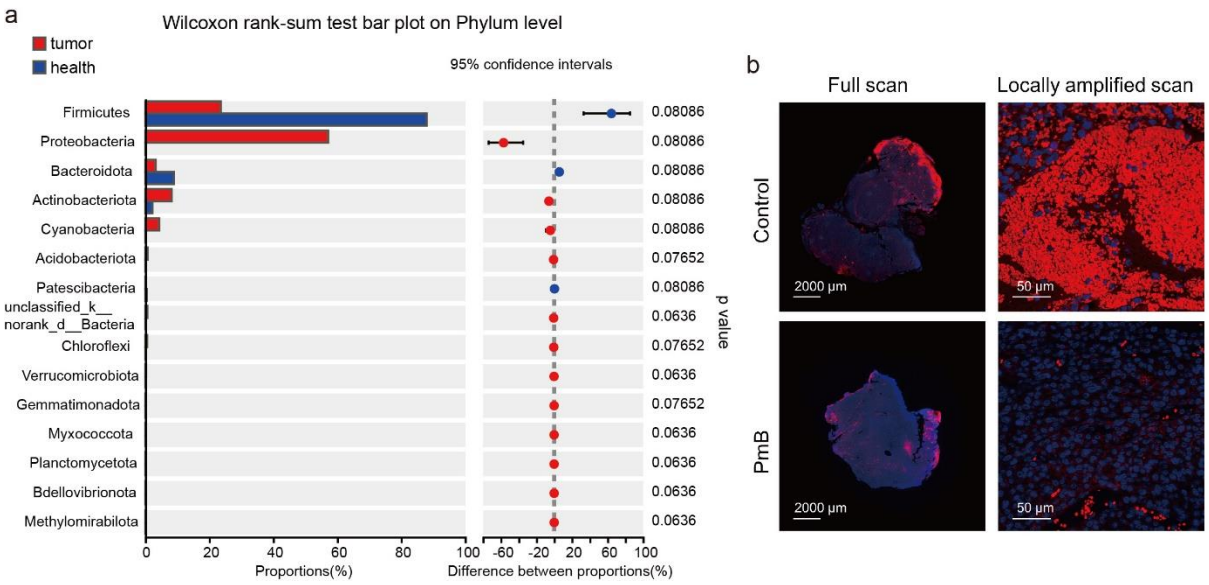

Supplementary Fig. 2 Intratumour microbiota changes after antibiotic treatment. a Microbiota at the Phylum level in pancreatic tumors and healthy pancreases identified by 16S rDNA analysis (n = 3 samples). **b** Intratumor microbes demonstrated by FISH staining after treated by PmB. Both full scan and locally amplified scan were showed (The bacteria were stained into red). Experiments were repeated three times. n = 6 mice in each group.

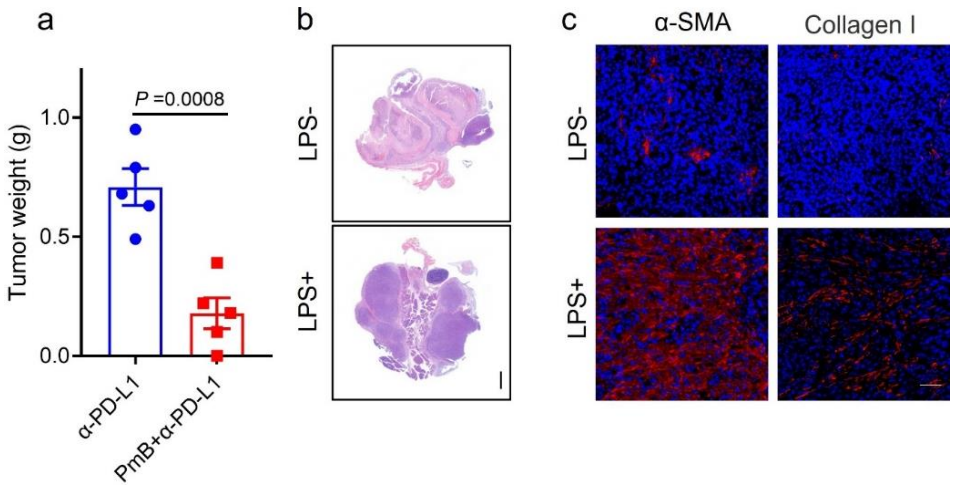

Supplementary Fig. 3 Assessment of in vivo antitumour effect. a Tumor weight in the KPC mice treatment with α-PD-L1 or α-PD-L1 plus PmB (n = 5 mice). **b** H&E staining and **c** α-SMA and Collagen I staining of tumor tissues with or without LPS treatment. The scale bar for (b) is 500 μm, and (c) is 200 μm. In **b**, **c**, experiments were repeated three times with n = 5 mice in each group. Significance between two groups was calculated using two-tailed Student's t-tests. Data are means ± sem. Source data are provided as a Source Data file.

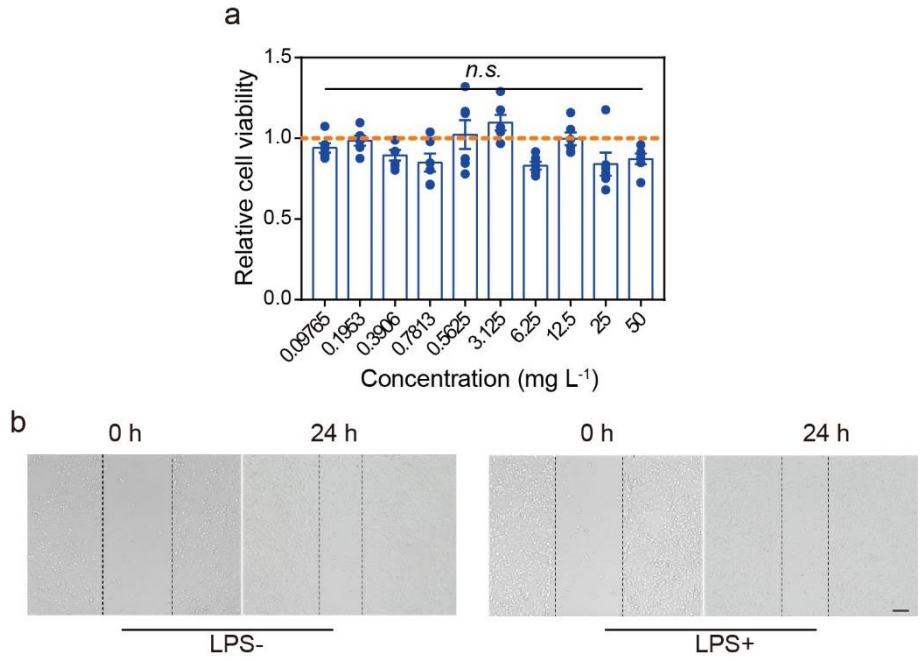

Supplementary Fig. 4 *In vitro* effect of LPS. **a** Cytotoxicity of different concentration of LPS on Panc-02 cells (n = 6 samples). **b** Cell migration after 24 h with and without LPS treatment. The scale bar is 100 μm. Experiments were performed three times with similar results. Significance between two groups was calculated using one-way ANOVA with Tukey post hoc test. Data are means ± sem. *n.s.* means no significance. Source data are provided as a Source Data file.

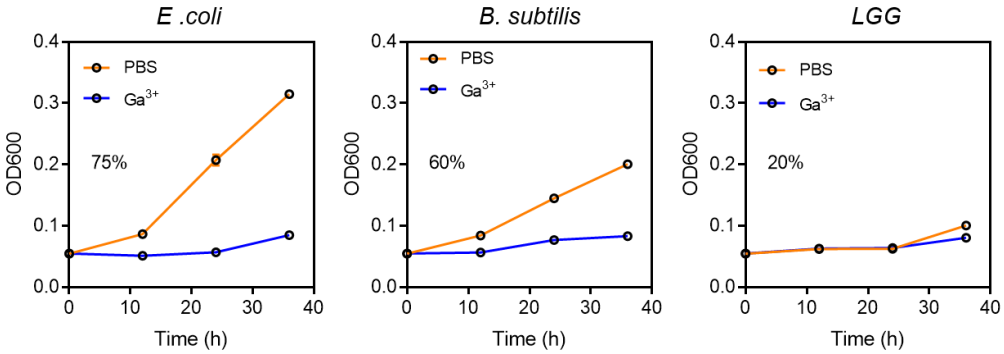

Supplementary Fig. 5 The bacterial growth after Ga^{3+} treatment in different time points. Three strains of bacteria were investigated. The antimicrobial efficacy of Ga^{3+} on *E. coli*, *B. subtilis*, and LGG are 75%, 60%, and 20%, respectively ($n = 6$ samples). Data are means ± sem. Source data are provided as a Source Data file.

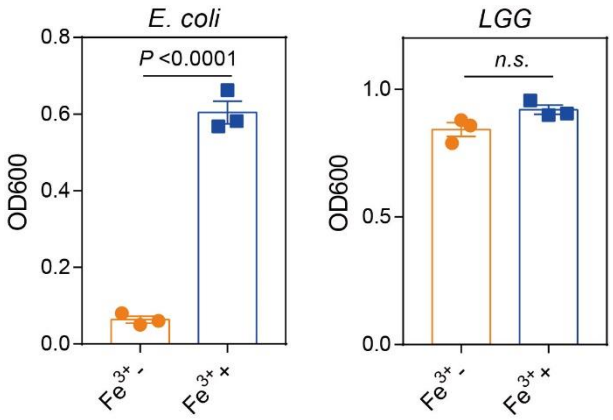

Supplementary Fig. 6 Growth of *E. coli* and LGG in the Fe^{3+}-added medium or medium without Fe^{3+} ($n = 3$ samples). Significance between two groups was calculated using two-tailed Student's t-tests. Data are means ± sem. *n.s.* means no significance. Source data are provided as a Source Data file.

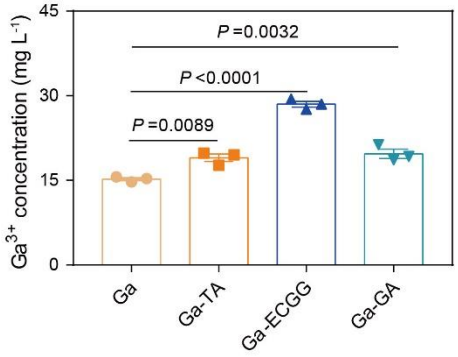

Supplementary Fig. 7 Concentration of Ga^{3+} ingested by bacterial cells when bacteria were incubated with Ga^{3+} or Ga^{3+} coordinated with various polyphenols (n = 3 samples). Significance between two groups was calculated using one-way ANOVA with Tukey post hoc test. Data are means ± sem. Source data are provided as a Source Data file.

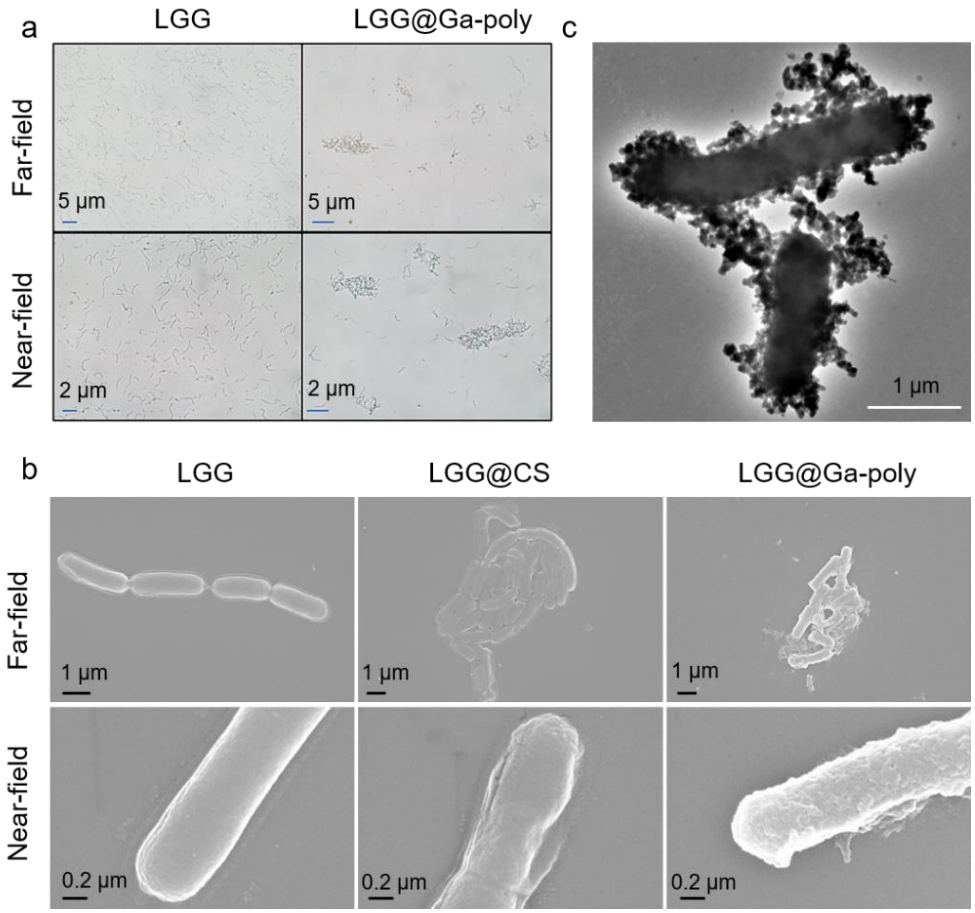

Supplementary Fig. 8 The morphological observation of LGG@Ga-poly. **a** Representative bright-field images of LGG and LGG@Ga-poly. **b** SEM images of LGG, LGG@CS, and LGG@Ga-poly. **c** TEM image of LGG@Ga-poly. Experiments were performed three times (**a**-**c**).

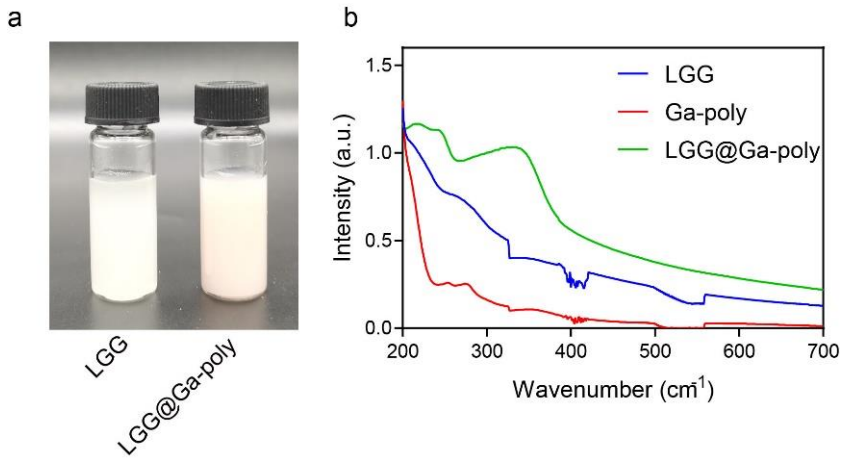

Supplementary Fig. 9 Characterization of LGG@Ga-poly. a Bright-field images of LGG and LGG@Ga-poly in PBS. Experiments were performed three times. **b** UV-*vis* spectra of LGG, Ga-poly, and LGG@Ga-poly. Experiments were performed three times with similar results. Source data are provided as a Source Data file.

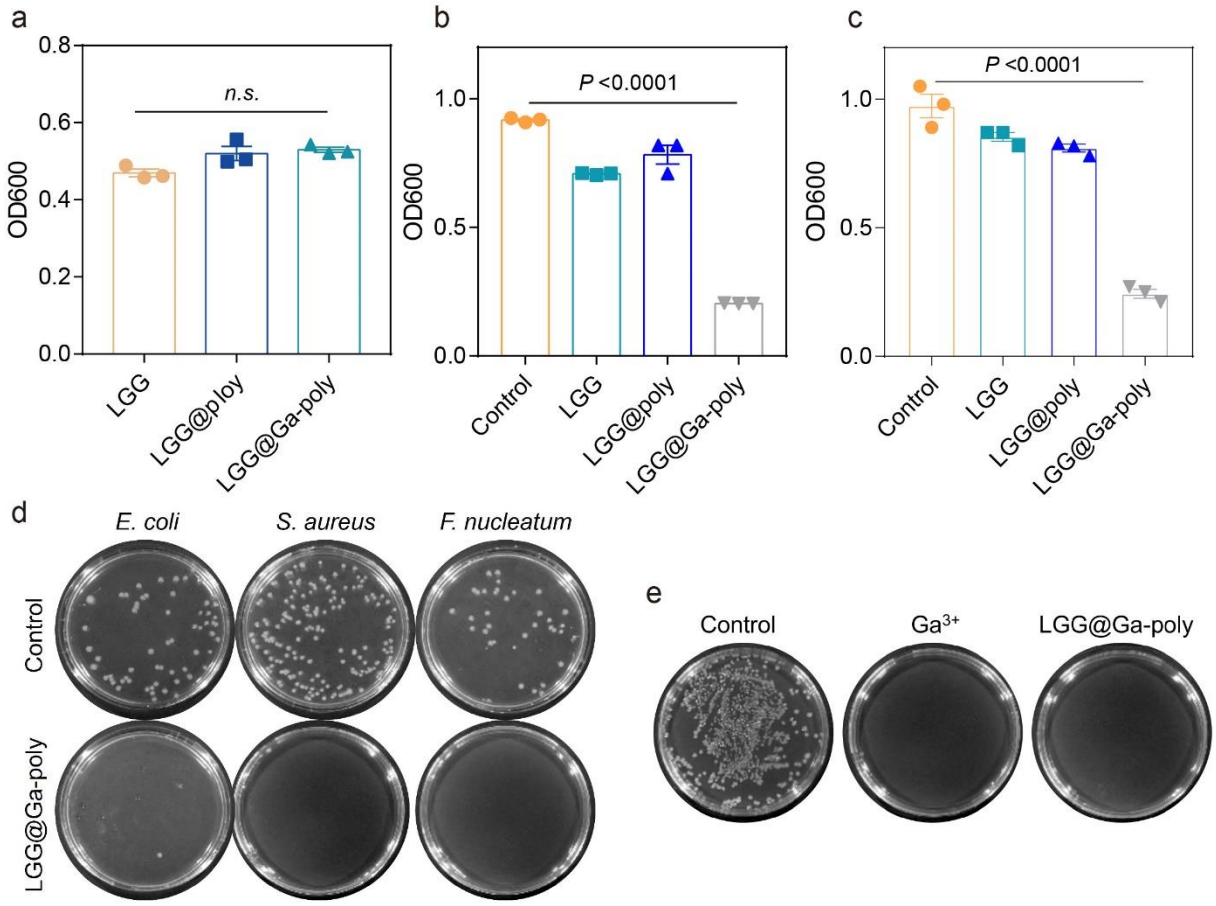

Supplementary Fig. 10 In vitro evaluation of antibacterial properties. a LGG viability in the SCF treated with different materials, including LGG, LGG@poly, and LGG@Ga-poly (*n* = 3 samples). The growth of **b** *E. coli* and **c** *S. aureus* after different treatments (*n* = 3 samples). **d** Bacterial growth on agar plates after treated by LGG@Ga-poly. Three bacterial strains, including *E. coli*, *S. aureus*, and *F. nucleatum*, were used for evaluation. **e** In a *F. nucleatum* - infected cell model, the bacterial colonies of *F. nucleatum* on agar plates after different treatments. In **d**, **e**, experiments were repeated three times with *n* = 3 samples in each group. Significance between two groups was calculated using one-way ANOVA with Tukey post hoc test. Data are means ± sem. *n.s.* means no significance. Source data are provided as a Source Data file.

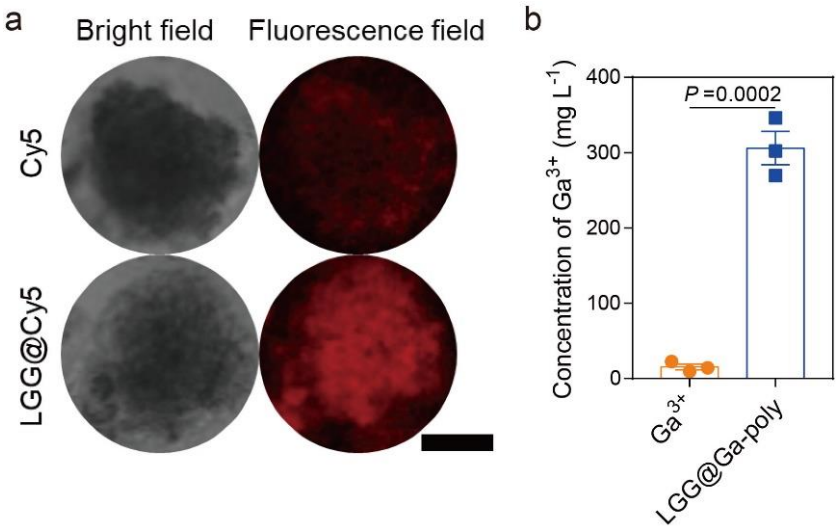

Supplementary Fig. 11 Penetration capability of LGG@Ga-poly. a Penetration of Cy5 and LGG@Cy5 into the 3D PDA cell spheres. Both bright-field and fluorescence-field images are shown. The scale bar is 50 μm. Experiments were repeated three times (n = 3 samples). **b** Concentration of Ga^{3+} in the cell spheres treated with Ga^{3+} and LGG@Ga-poly (n = 3 samples). Significance between two groups was calculated using two-tailed Student's t-tests. Data are means ± sem. Source data are provided as a Source Data file.

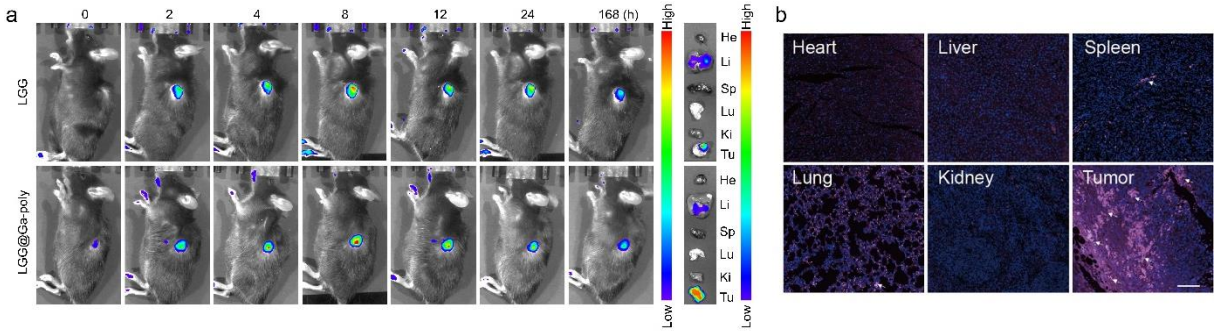

Supplementary Fig. 12 In vivo tumour-targeting of LGG@Ga-poly. a In vivo and ex vivo fluorescence imaging of orthotopic PDAC mice after oral administration of Cy5.5 labeled LGG or LGG@Ga-poly (A parallel repeat trial). He-heart, Li-liver, Sp-spleen, Lu-lung, Ki-kidney, Tu-tumor. **b** Histological fluorescence images of tumors and major organs following the oral administration of Cy5.5-labeled LGG@Ga-poly in PDAC mice. Arrows indicate LGG@Ga-poly. The scale bar is 50 μm. In **a**, **b**, experiments were repeated three times with $n = 3$ mice in each group.

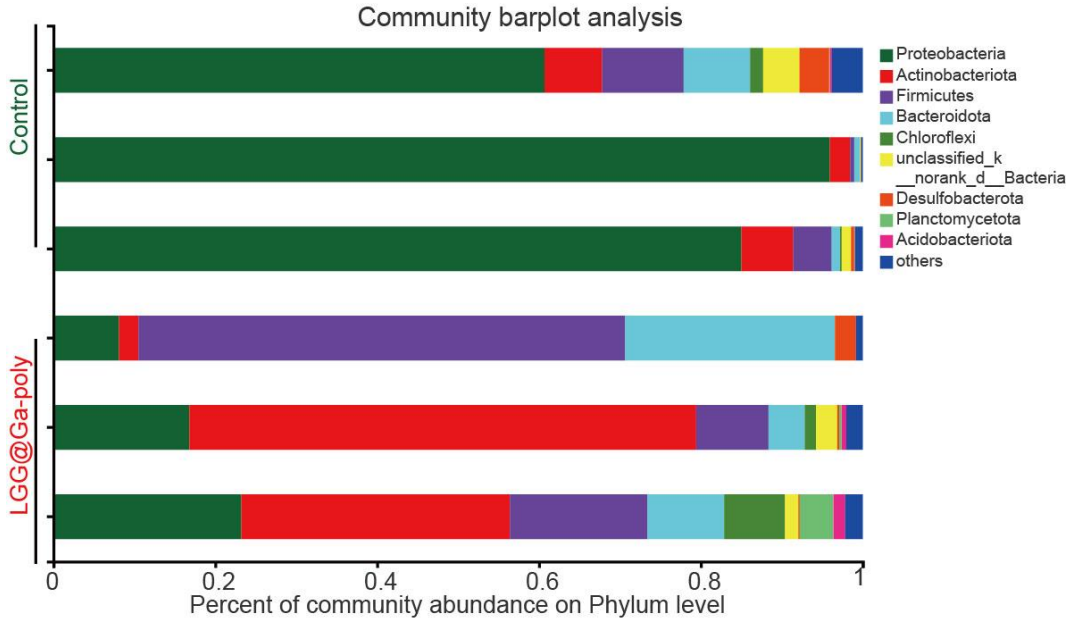

Supplementary Fig. 13 Relative abundances of the intratumor commensal microbes at the Phylum level in the control group and the LGG@Ga-poly treatment group ($n = 3$ samples)**.**

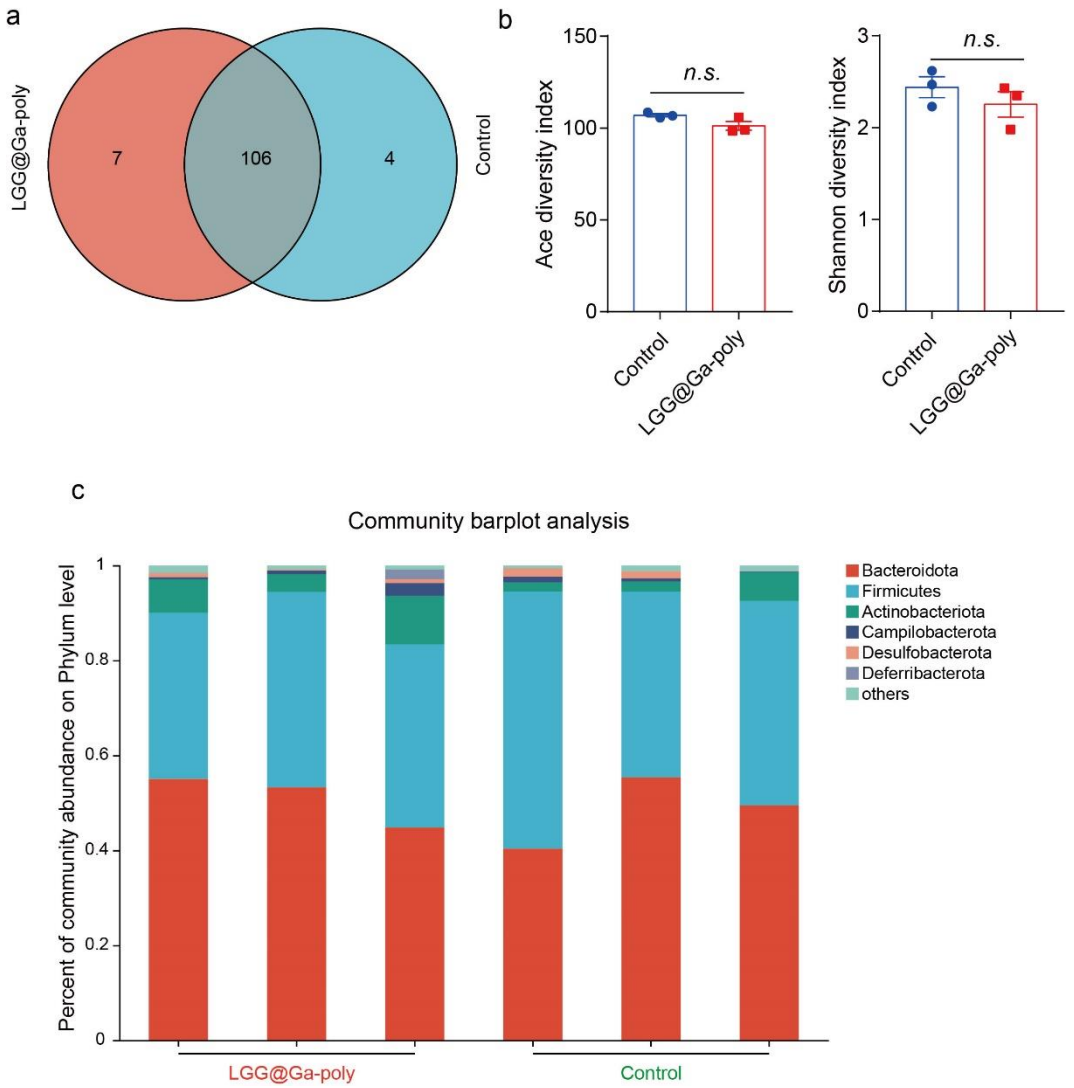

Supplementary Fig. 14 Changes of the gut commensal microbes treated by LGG@Ga-poly. **a** Venn diagram for the strains of identified gut bacteria in the control and LGG@Ga-poly treatment group (n = 3 samples). **b** The α-diversity of gut microbiota community (Ace and Shannon) in the control and LGG@Ga-poly treatment group (n = 3 samples). **c** Relative abundances of the gut commensal microbes at the Phylum level in the control and LGG@Ga-poly treatment group (n = 3 samples). Significance between two groups was calculated using two-tailed Student's t-tests. Data are means ± sem. *n.s.* means no significance. Source data are provided as a Source Data file.

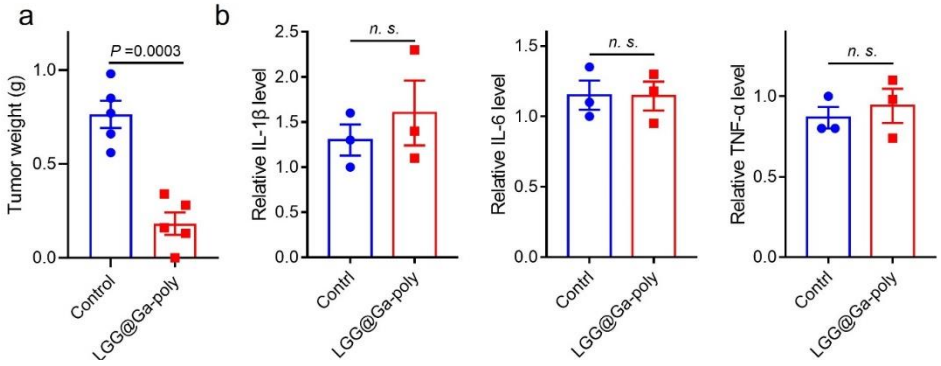

Supplementary Fig. 15 Tumor prevention capacitary and safety assessment. a Tumor weight after LGG@Ga-poly treatment in a prophylactic regimen (n = 5 mice). **b** The assessment of immune-related cytokines in the blood of healthy mice after LGG@Ga-poly treatment. LGG@Ga-poly was orally administrated to healthy mice for three months and cytokines were detected (n = 3 samples). Significance between two groups was calculated using two-tailed Student's t-tests. Data are means ± sem. *n.s.* means no significance. Source data are provided as a Source Data file.

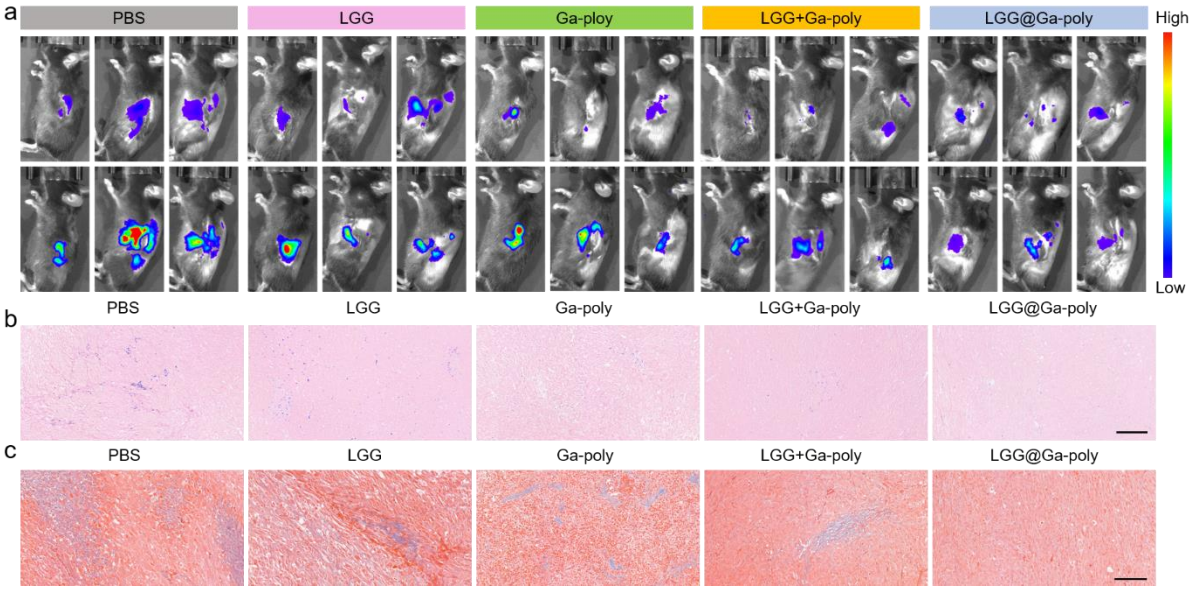

Supplementary Fig. 16 Therapeutic efficacy of different materials on the PDAC mice. **a** The whole-body bioluminescence imaging of PDAC mice after different treatments. Three representative mice images on both Day 7 (Top) and Day 28 (Bottom) are shown. *n* = 5 mice in each group. **b** The bacterial Gram staining of tumors in each group. The blue particles represent Gram-negative bacteria. The scale bar is 0.5 mm. **c** The Masson staining of tumors after different treatments. The blue areas represent collagen within tumors. The scale bar is 0.5 mm. In **b**, **c**, experiments were repeated three times with *n* = 5 mice in each group.

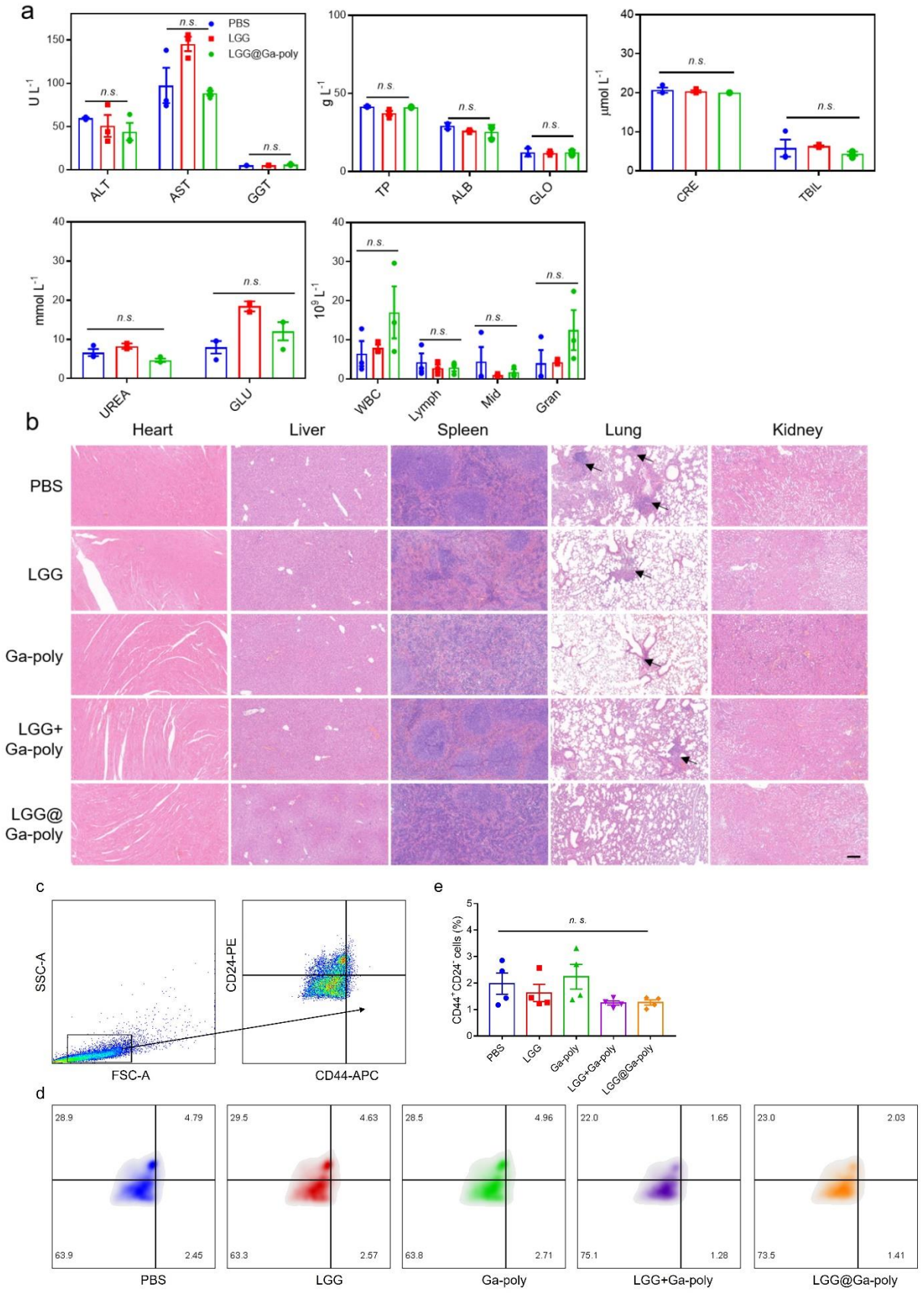

Supplementary Fig. 17 The biosafety evaluation of LGG@Ga-poly treatment on the PDAC mice. **a** Liver function test (ALT, AST, GGT, TP, ALB and GLO), kidney function test

(CRE, TBIL, UREA and GLU), and hematological examination (WBC, Lymph, Mid, and Gran) after different treatments (n = 3 samples). **b** H&E images of major organs after different treatments. The scale bar is 0.5 mm. Arrows indicate metastatic tumor niches. Experiments were performed three times. n = 5 mice in each group. FCM analysis of $CD44^{+}CD24^{-}$ cancer stem cells in the tumor. Gating strategy **c**, FCM images **d** and quantitative analysis **e** of cancer stem cells after different treatments (n = 4 samples). Significance between two groups was calculated using one-way ANOVA with Tukey post hoc test. Data are means ± sem. *n.s.* means no significance. Source data are provided as a Source Data file.

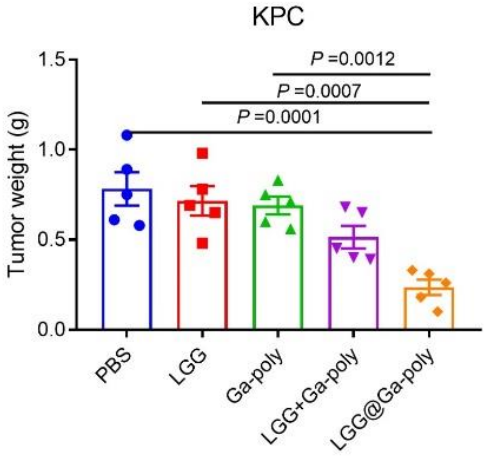

Supplementary Fig. 18 Tumor weight in the KPC mouse model after different treatments in a therapeutic setting (n = 5 mice). Significance between two groups was calculated using one-way ANOVA with Tukey post hoc test. Data are means ± sem. Source data are provided as a Source Data file.

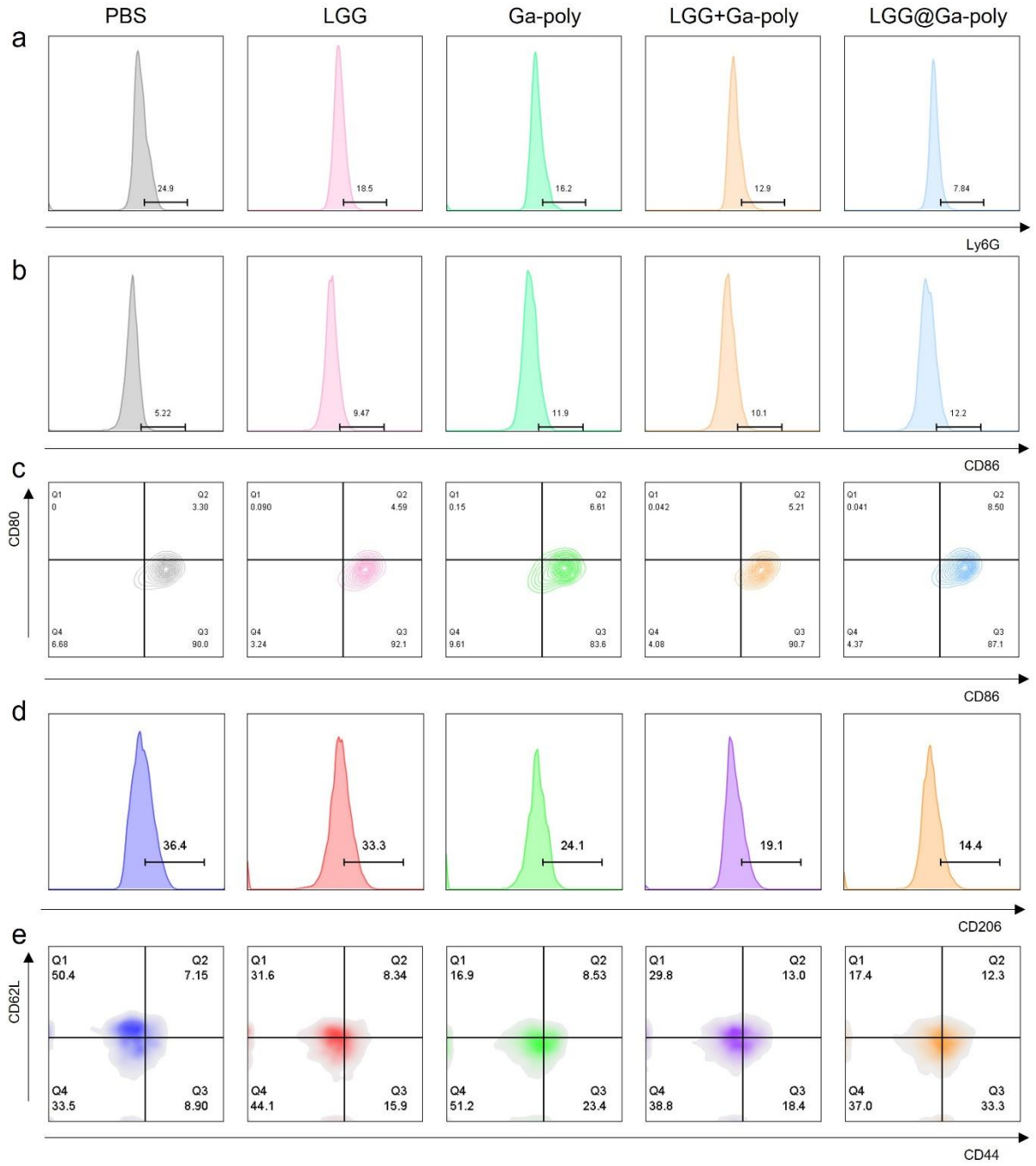

Supplementary Fig. 19 Representative FCM images for immune cells after different treatment. FCM images of $CD11b^+Ly6G^+$ MDSC cells **a** $CD11b^+CD86^+$ M1 cells **b** within tumors after different treatments; $CD11c^+CD80^+CD86^+$ DC cells **c** within lymph nodes; $CD11b^+CD206^+$ M2 cells **d** within tumors and $CD3^+CD8^+CD44^+$ $CD62L^-$ T_{EM} cells **e** within spleens after different treatments. $n = 4$ samples.

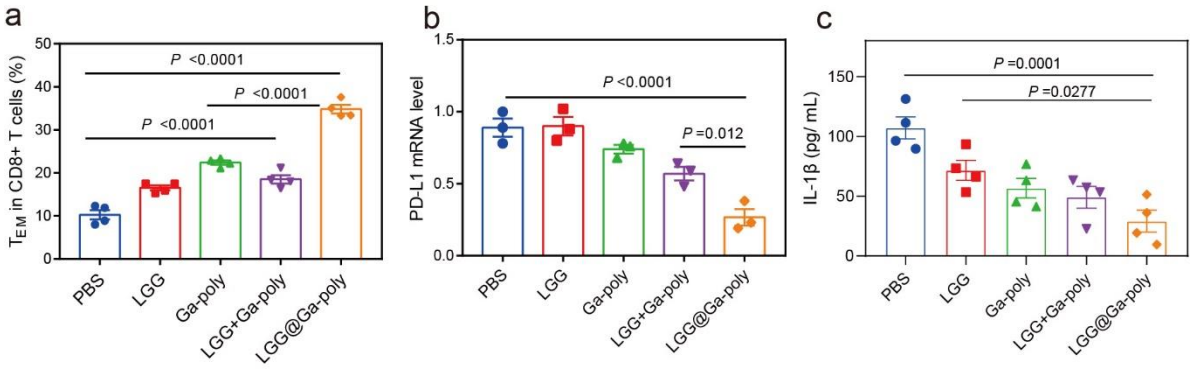

Supplementary Fig. 20 Immune analysis in each group. a $CD3^+CD8^+CD44^+CD62L^-$ T_{EM} cells in the spleen (n = 4 samples). **b** Relative PD-L1 mRNA level of tumor tissues in each group (n = 3 samples). **c** ELISA detections indicated the concentrations of pro-tumor IL-1β in the tumors after different treatments (n = 4 samples). Significance between two groups was calculated using one-way ANOVA with Tukey post hoc test. Data are means ± sem. Source data are provided as a Source Data file.

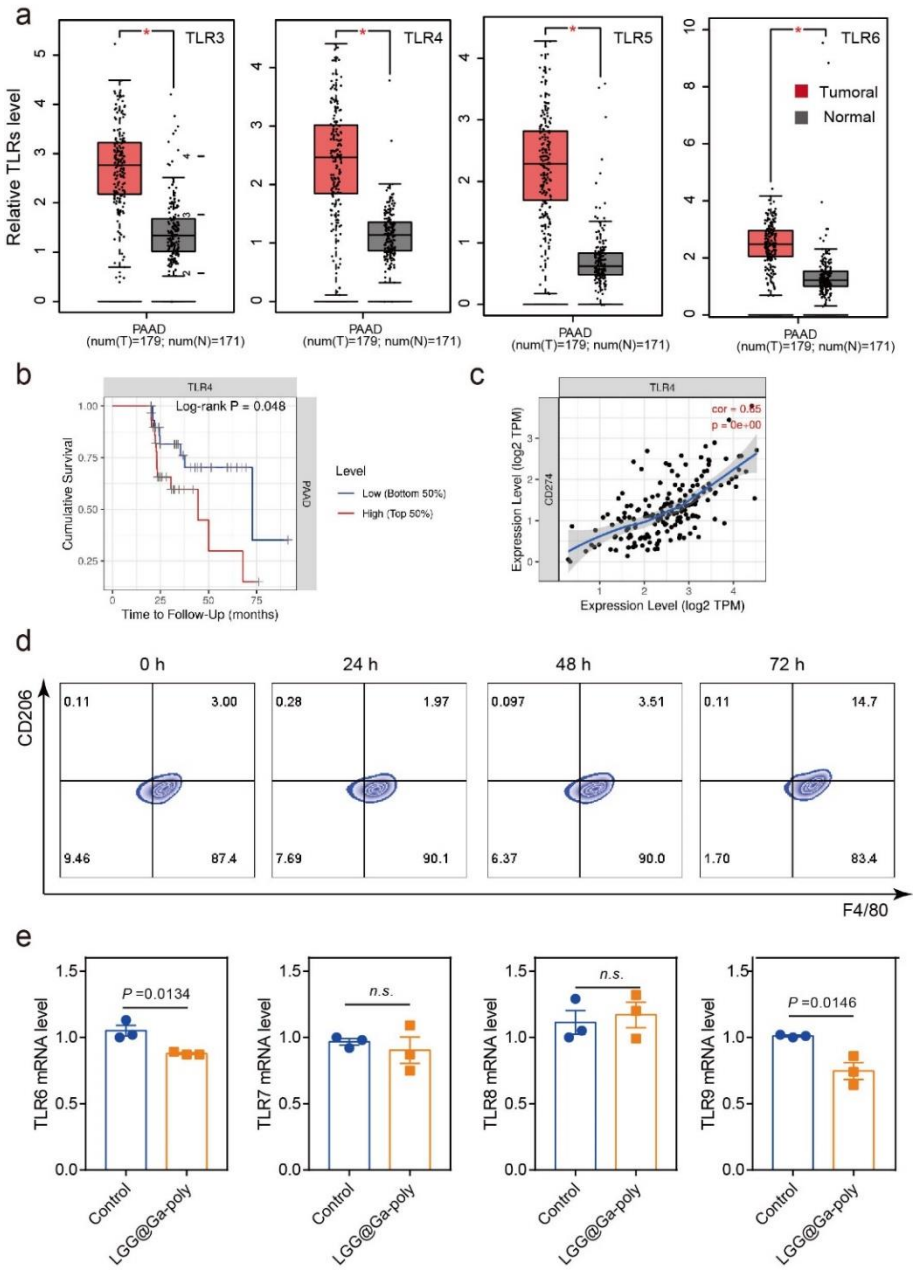

Supplementary Fig. 21 The TLRs-dependent immune-activation by LGG@Ga-poly. **a** TLR3-TLR6 expressions in pancreatic tumors of PDAC patients and normal pancreas analyzed by TCGA database. **b** The correlation between tumor TLR4 expression and survival time of PDAC patients analyzed by TCGA database (Low (*n*)= 89 patients, High (*n*)= 89 patients). **c** The correlation between TLR4 expression and CD274 (PD-L1) expression analyzed by TCGA database (*n* = 178 patients). **d** FCM images of $F4/80^{+}CD206^{+}$ M2 cells when RAW264.7 cells were treated by LPS for different time points. **e** TLR6-TLR9 expressions in pancreatic tumors treated by LGG@Ga-poly (*n* = 3 samples). Significance between two groups was calculated using two-tailed Student's t-tests (e). Data are means ± sem. *n.s.* means no significance. Source data are provided as a Source Data file.

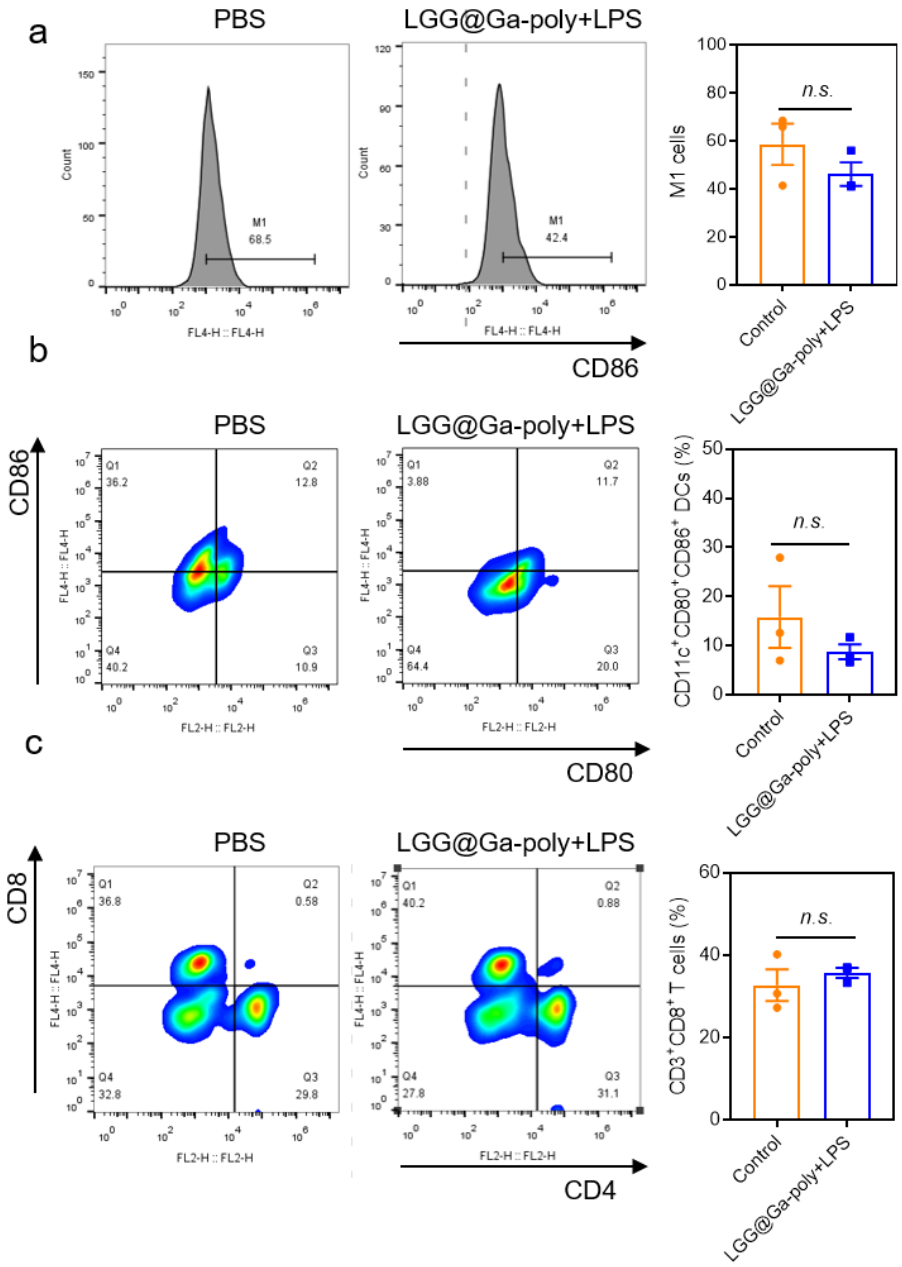

Supplementary Fig. 22 FCM images and quantitative analyses of immune cells after treated by LGG@Ga-poly + LPS. **a** FCM images and quantitative analysis of M1 cells in the tumors (n = 3 samples). **b** FCM images and quantitative analysis of DC cells in the lymph nodes (n = 3 samples). **c** FCM images and quantitative analysis of $CD3^+CD8^+$ T cells in the spleens (n = 3 samples). Significance between two groups was calculated using two-tailed Student's t-tests. Data are means ± sem. *n.s.* means no significance. Source data are provided as a Source Data file.

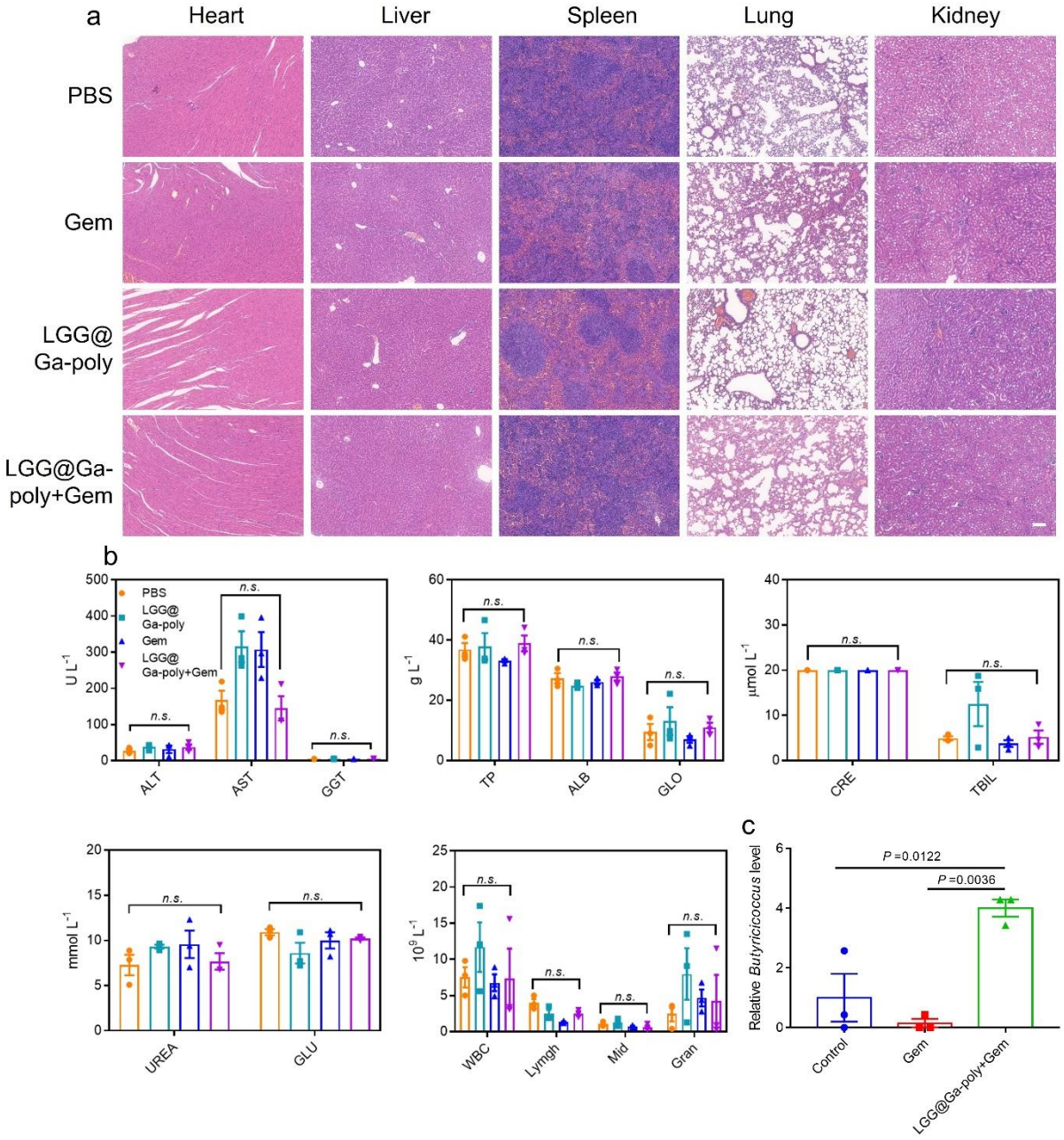

Supplementary Fig. 23 In vivo safety assessment. a H&E images of major organs in the orthotopic PDAC mice model after treated by PBS, Gem, LGG@Ga-poly, and LGG@Ga-poly + Gem. The scale bar is 0.1 mm. Experiments were performed three times. n = 5 mice in each group. **b** Biosafety evaluation of LGG@Ga-poly combined with chemotherapy in the orthotopic PDAC mice model (n = 3 samples). **c** Relative *Butyricicoccus* level in the gut after different treatments (n = 3 samples). Significance between two groups was calculated using one-way ANOVA with Tukey post hoc test. Data are means ± sem. *n.s.* means no significance. Source data are provided as a Source Data file.

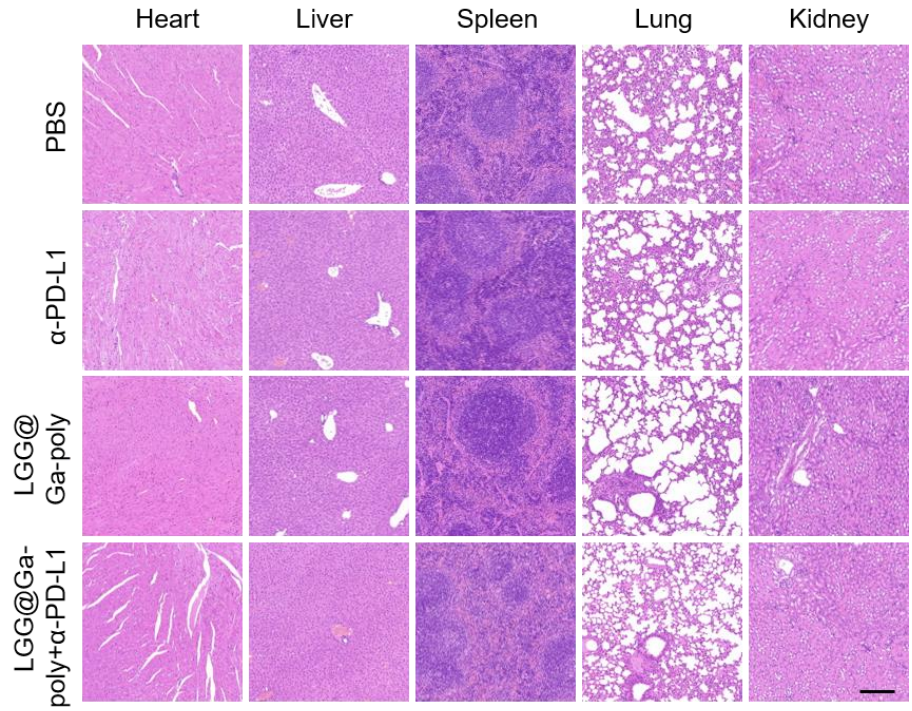

Supplementary Fig. 24 H&E images of major organs in the orthotopic PDAC mice model after treated by PBS, α-PD-L1, LGG@Ga-poly, and LGG@Ga-poly + α-PD-L1. The scale bar is 0.5 mm. Experiments were performed three times. *n* = 6 mice in each group.

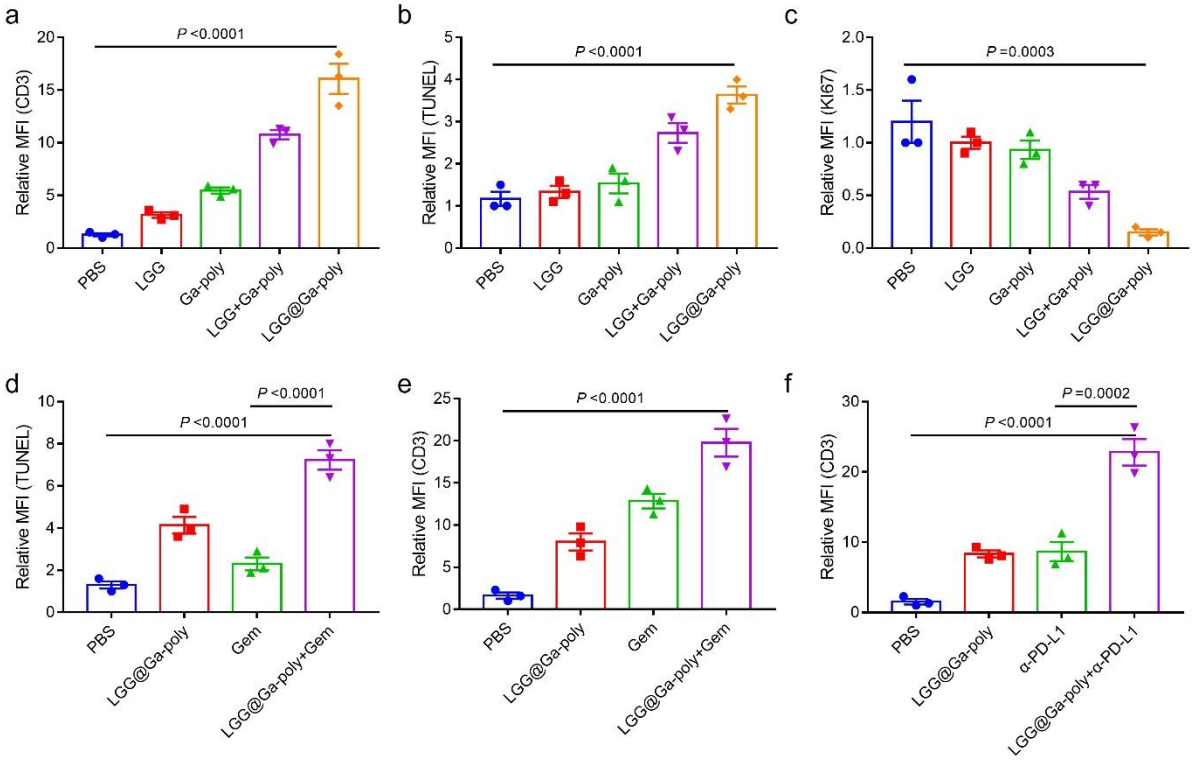

Supplementary Fig. 25 The quantification of the immunofluorescence staining data for *Figure 5e* (a), *5k* (b, c), *8d* (d), *8e* (e), *8k* (f). $n = 3$ samples. Significance between two groups was calculated using one-way ANOVA with Tukey post hoc test. Data are means ± sem. Source data are provided as a Source Data file.

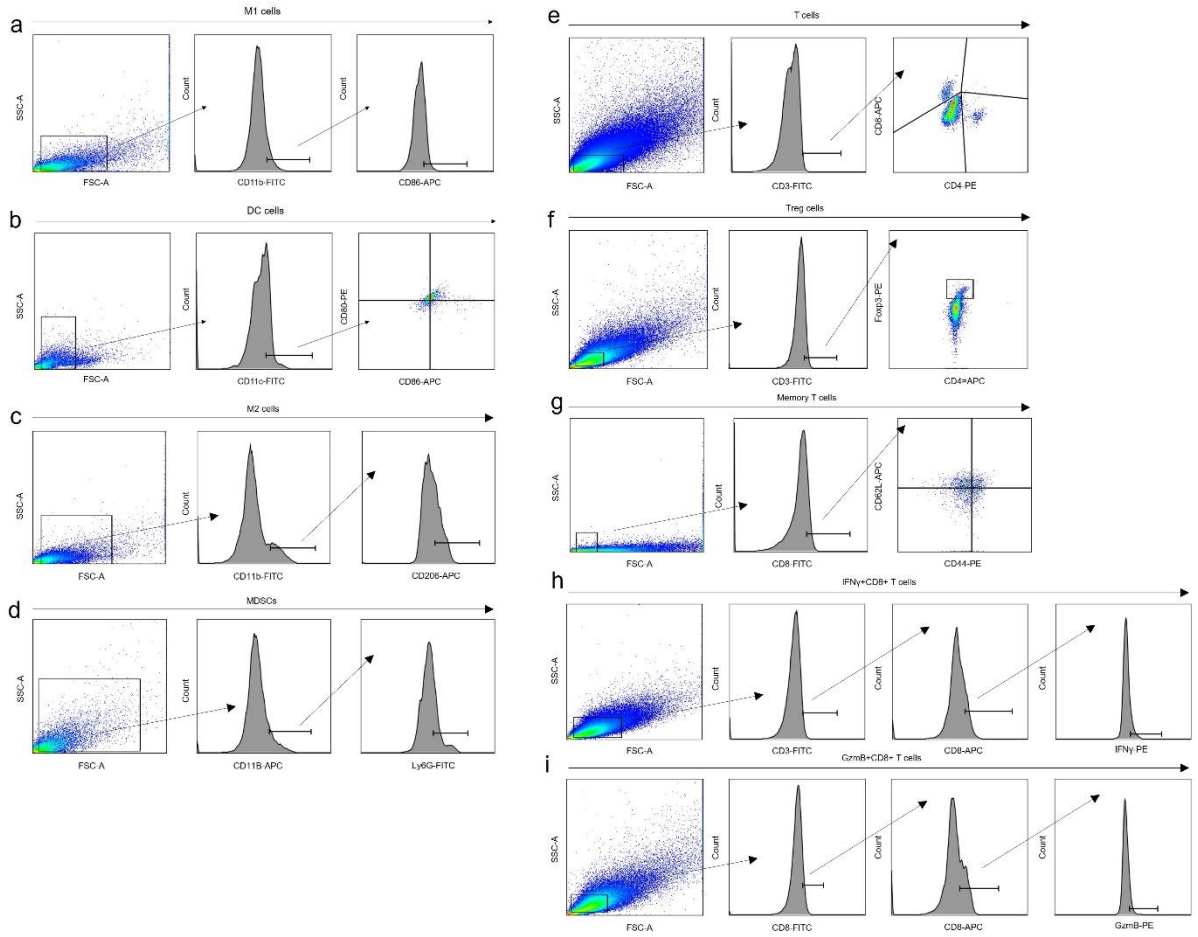

Supplementary Fig. 26 The gating strategy. a The gating strategy for M1-like macrophages used in Fig 2i, Fig 6b, Supplementary Fig 22a; **b** The gating strategy for DC cells used in Fig 2i, Fig 6a, Supplementary Fig 22b; **c** The gating strategy for M2-like macrophages used in Fig 2i, Fig 6d; **d** The gating strategy for MDSCs used in Fig 2i, Fig 6e; **e** The gating strategy for T cells used in Fig 2i, Fig 6f, Fig 7g, Supplementary Fig 22c; **f** The gating strategy for Treg cells used in Fig 6g; **g** The gating strategy for memory T cells used in Supplementary Figs 19e, 20a; **h** The gating strategy for $IFN\gamma^{+}CD8^{+}$ T cells used in Fig 6i; **i** The gating strategy for $GzmB^{+}CD8^{+}$ T cells used in Fig 6h.